AMERICAN SOCIETY FOR MICROBIOLOGY | mBio

| Mycology | Research Article

Mucor germinans, a novel dimorphic species resembling *Paracoccidioides* in a clinical sample: questions on ecological strategy

Na Li,[1,2,3] Jennifer Bowling,[4] Sybren de Hoog,[1,2,3] Chioma I. Aneke,[4] Jung-Ho Youn,[4] Sherin Shahegh,[4] Jennifer Cuellar-Rodriguez,[5] Christopher G. Kanakry,[6] Maria Rodriguez Pena,[7] Sarah A. Ahmed,[3] Abdullah M. S. Al-Hatmi,[8] Ali Tolooe,[9,10] Grit Walther,[11] Kyung J. Kwon-Chung,[5] Yingqian Kang,[1,2,12] Hyang Burm Lee,[13] Amir Seyedmousavi[4]

AUTHOR AFFILIATIONS See affiliation list on p. 15.

ABSTRACT Dimorphism is known among the etiologic agents of endemic mycoses as well as in filamentous *Mucorales*. Under appropriate thermal conditions, mononuclear yeast forms alternate with multi-nucleate hyphae. Here, we describe a dimorphic mucoralean fungus obtained from the sputum of a patient with Burkitt lymphoma and ongoing graft-versus-host reactions. The fungus is described as *Mucor germinans* sp. nov. Laboratory studies were performed to simulate temperature-dependent dimorphism, with two environmental strains *Mucor circinelloides* and *Mucor kunryangriensis* as controls. Both strains could be induced to form multinucleate arthrospores and subsequent yeast-like cells *in vitro*. Multilateral yeast cells emerge in all three *Mucor species* at elevated temperatures. This morphological transformation appears to occur at body temperature since the yeast-like cells were observed in the lungs of our immunocompromised patient. The microscopic appearance of the yeast-like cells in the clinical samples is easily confused with that of *Paracoccidioides*. The ecological role of yeast forms in *Mucorales* is discussed.

IMPORTANCE Mucormycosis is a devastating disease with high morbidity and mortality in susceptible patients. Accurate diagnosis is required for timely clinical management since antifungal susceptibility differs between species. Irregular hyphal elements are usually taken as the hallmark of mucormycosis, but here, we show that some species may also produce yeast-like cells, potentially being mistaken for *Candida* or *Paracoccidioides*. We demonstrate that the dimorphic transition is common in *Mucor* species and can be driven by many factors. The multi-nucleate yeast-like cells provide an effective parameter to distinguish mucoralean infections from similar yeast-like species in clinical samples.

KEYWORDS *Mucor germinans* sp. nov., *Mucor circinelloides*, dimorphism, mucormycosis, *Paracoccidioides*

Mucormycosis is an aggressive opportunistic infection with high morbidity and mortality in humans. Classically, the infection occurs at low frequency in patients with diabetic ketoacidosis or hematological malignancies (1, 2). A significant increase in infections due to *Mucorales*, termed COVID-19-associated mucormycosis, was observed during the recent COVID-19 pandemic in patients with uncontrolled diabetes and overuse of steroids (3–5). The species causing mucormycosis are members of the order *Mucorales*, with *Rhizopus* and *Lichtheimia* isolated more frequently than *Mucor* species (1, 2, 6). The main routes of infection by mucoralean fungi are by inhalation of airborne spores or by inoculation into disrupted skin or gastrointestinal mucous membranes (2, 7, 8). The lungs, skin, soft tissues, and paranasal sinus/sino-orbital and rhino-cerebral

Editor Tom Chiller, CDC, Atlanta, Georgia, USA

Address correspondence to Yingqian Kang, kangyingqian@gmc.edu.cn, Hyang Burm Lee, hblee@jnu.ac.kr, or Amir Seyedmousavi, seyedmousavi@nih.gov.

Na Li and Jennifer Bowling contributed equally to this article. The order was decided based on the contribution to the article.

The authors declare no conflict of interest.

See the funding table on p. 15.

Received 16 January 2024
Accepted 30 May 2024
Published 2 July 2024

regions are the main sites of infection (7). Due to the rapid progression and high mortality rate of mucormycosis, early diagnosis and appropriate antifungal therapy are critical for improved clinical outcomes and patient survival (1, 9).

Given the acute progression of mucoralean infections and different levels of antifungal resistance between species, rapid identification of the agent is critical (2, 3). Since isolation and culture from infected sites are difficult, direct microscopy and histopathology of various clinical specimens are the basis of the diagnosis of mucormycosis (2, 10). Hyphae can be visualized with optical brighteners such as Blankophor (11) or Calcofluor white/Fungi-Fluor staining (12). Hyphae of *Mucorales* in infected tissues are non-septate or pauci-septate with an irregular, ribbon-like appearance (13, 14). However, there have been case reports where mucoralean agents presented in a yeast-like form in the clinical specimens (15). Several authors reported the presence of yeast-like forms in direct microscopic examination of urine, vaginal, and tracheal samples, e.g., in infections caused by *Cokeromyces recurvatus* (16, 17).

In the course of the present study, an unknown dimorphic mucoralean fungus was observed in the sputum of a patient with a history of Burkitt lymphoma, who had undergone allogeneic bone marrow transplantation. The fungus presented as multilateral budding cells, which were predominant upon direct microscopic examination of sputum samples; no hyphae were observed. Daughter cells were attached to the mother cell with broad flat bases, resembling the budding of *Paracoccidioides* species. This evidence suggests that yeast-like cell morphology *in situ* might be an overlooked feature among the clinical samples of *Mucorales*. This unexpected appearance of *Mucorales* in the host may significantly delay the diagnosis and treatment of mucormycosis as long as additional diagnostic evidence is missing.

In *Mucorales*, yeast-like forms have mainly been described in the genus *Mucor* (18–22). The ecological advantage of dimorphism in these fungi was thought to enhance survival in liquid habitats requiring alternation of their thallus organization to unicellularity (22). Dimorphic strategies are widely applied in plant and animal pathogenic fungi where encounter with the host prompts a shift in the mode of growth (23). Factors enhancing mold-to-yeast conversion differ between fungal groups. For *Paracoccidioides brasiliensis*, the change from ambient temperature of 25°C to host temperature of 37°C is sufficient (24), but for *Sporothrix* species and *Talaromyces marneffei*, additives are required (25, 26). In the family *Ajellomycetaceae*, to which *Paracoccidioides* belongs, the preponderantly environmental fungi show more reluctant conversion (27).

Dimorphic transition in *Mucorales* has been studied mainly in *Mucor circinelloides* (28–30), but the phenomenon occurs more widely in the genus *Mucor* (31). With the increasing occurrence of *Mucorales* in the clinic as pulmonary colonizers or causative agents of mucormycosis and given the acute and fulminant features of infections such as rhinocerebral mucormycosis (32), the yeast-mycelium transformation and its relationship with temperature and host conditions require further study.

The present work was prompted by the occurrence of yeast cells with morphological similarity to *Paracoccidioides* in the sputum of an immunocompromised patient. Additional morphological, phylogenetic, and physiological analyses revealed the fungus to be a new species of *Mucor*. *In vitro* experiments were conducted to determine the factors that induce the formation of yeast cells in comparison with *M. circinelloides* and *M. kunryangriensis,* which show temperature-dependent conversion.

RESULTS

Isolation of clinical strain

A sputum sample from a 32-year-old patient with Burkitt lymphoma, who was 35 days post-allogeneic bone marrow transplant, was collected at the Microbiology Service of Department of Laboratory, NIH Clinical Center, Bethesda, MD, USA. The patient was receiving posaconazole infusion prophylaxis given his post-transplant status and ongoing reactions of graft-versus-host disease treated with methylprednisolone, tacrolimus, and ruxolitinib. The patient was afebrile at the time of sample collection,

and the sputum sample was obtained due to CT chest imaging the day prior showing interval development of patchy ground-glass opacities throughout the lungs, some areas of which are nodular in configuration. The sputum sample was Gram-stained and evaluated microscopically. The sample showed abundant squamous epithelial cells, mixed oropharyngeal flora, and rare neutrophils. In addition, yeast-like cells were observed, with large, spherical mother cells giving rise to spherical budding cells with multilateral production of daughter cells, which were inserted into the mother cell at a rather broad base (Fig. 1).

Presumptive identification on the basis of the microscopic appearance suggested a fungus close to *Paracoccidioides*. A portion of the sputum specimen was separated aseptically, inoculated repeatedly onto Sabouraud glucose agar (SGA), and incubated at 30°C. After 2 days, rapidly growing, cottony to fluffy, white to yellow colonies (Fig. 2) appeared with the development of sporangia. This mucoralean-like fungus was stored at −80°C under number SM1517. No yeast-like fungus was isolated on any occasion.

MALDI-ToF MS

Three *Mucor* species including the clinical isolate *M. germinans* (SM1517), *M. circinelloides* (CBS 151457), and *Mucor kunryangriensis* (CNUFC CY223) were analyzed by matrix-assisted laser desorption/ionization time-of-flight mass spectrometry (MALDI-ToF MS) in duplicate. Profiles with more than 80 peaks were considered as reliable results and were included for further analysis. No match was obtained with any of the profiles stored in the MALDI Biotyper (Bruker Daltonics Inc.) and NIH Bruker Daltonics databases for *M. germinans* (SM1517 and CBS 151458), and *M. kunryangriensis* (CNUFC CY223); all spectra yielded scores of <1.7.

Mass spectra obtained from each tested *Mucor* species were compared to each other, and for each species, a main spectrum (MSP) was created (Fig. S1). Accurate analysis with FlexAnalysis software (version 3.4, Bruker Daltonics Inc.) highlighted several discriminating peaks between *M. germinans*, *M. circinelloides,* and *M. kunryangriensis*. The MSP of these species resulted to be differentiable based on their overall peak number, consistent for each *Mucor* species.

Direct PCR sequencing of sputum sample

Comparison of the internal transcribed spacer (ITS) sequence (577 nucleotides) to both databases yielded a sequence identity of <94% to the type strain of *M. cheongyangensis* (*Mucor* sp. isolate CNUFC ICL1), but these data were considered insufficient to conclude the species level of this isolate.

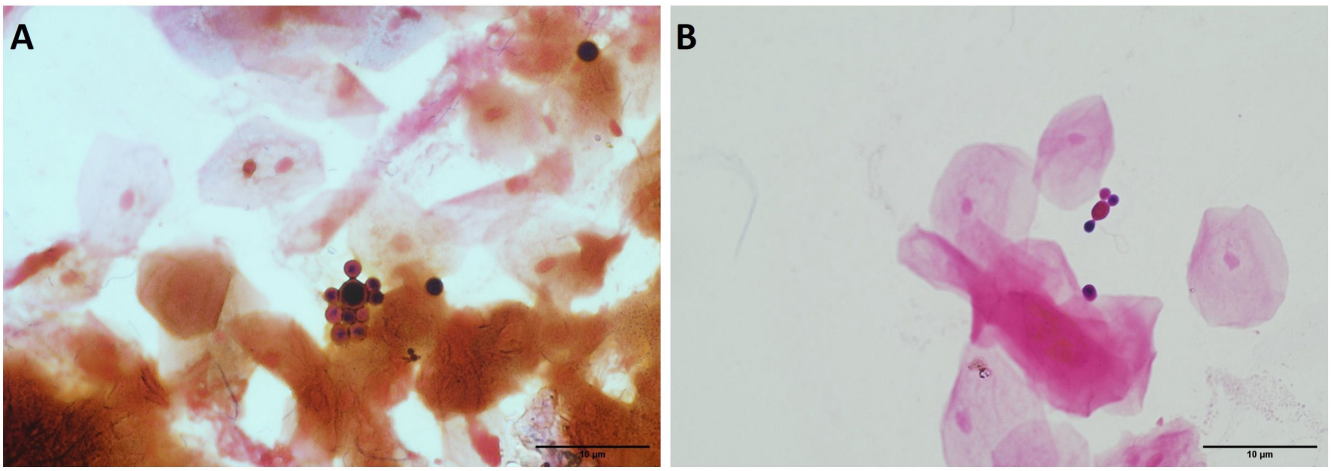

FIG 1 Direct microscopic examination of the sputum (Gram stain) with yeast phase resembling *Paracoccidioides*. (A) Multiple spherical buds all over the surface, (B) "Mickey Mouse" shaped budding structure. Scale bar: 10 µm.

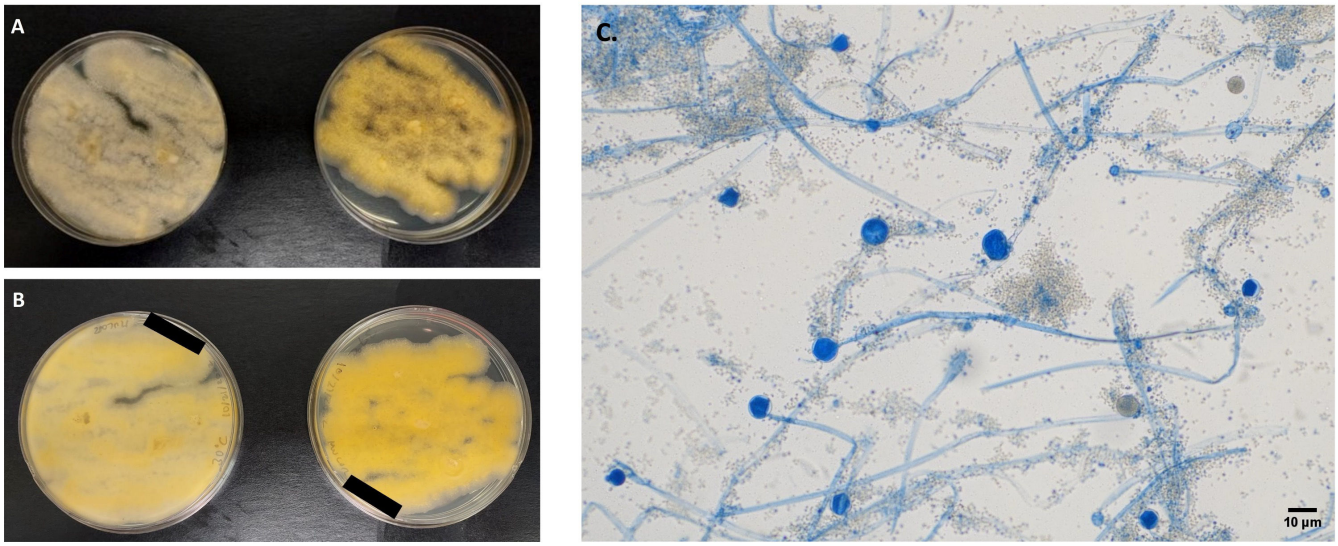

FIG 2 Macroscopy and microscopy characteristics of *Mucor germinans* sp. nov. (A) Colony morphology on Sabouraud glucose agar at 30°C (left) and 37°C (right). (B) Reverse of colonies at 30°C (left) and 37°C (right). (C) Lactophenol cotton blue wet mount (10×) showing hyaline non-septate hyphae, sporangiophores, terminal globose, multi-spored sporangia, and columellae. Scale bar: 10 µm.

Phylogeny

To understand the evolutionary position of the *Mucor*-like fungus and its relationship with other dimorphic *Mucor* species, sequences of ITS were used for a phylogenetic analysis (Fig. 3). The ITS analyses revealed that the isolate SM1517 was related to *M. cheongyangensis* but formed a separate branch, and this distinction was supported by a high bootstrap value (100%). *M. circinelloides* grouped with numerous dimorphic *Mucor* species, but remote from the SM1517 strain. *M. kunryangriensis*, another dimorphic species, was positioned far from both the mucor-like species and *M. circinelloides*. On the basis of these data, the SM1517 strain was considered to represent a novel species as described below. The corresponding sequences for the SM1517 strain were submitted to GenBank (accession number: OQ709230.1).

Mucor germinans Na Li, Bowling, de Hoog, and Seyedmousavi, sp. nov. (Fig. 4)—MycoBank MB853494

Etymology: Latin *germinans* refers to the sprouting cells produced at 37°C.

Typus: Bethesda, USA, from the sputum of a human patient, 07 October 2022 (holotype CBS H-25350; Ex-type culture SM1517 = CBS 151458).

Description: Colonies on SGA attain a diameter of 80–86 mm after 4 days at 28°C, at first white and then becomes yellowish brown; colony reverse yellow to pale with shades of gray and brown (Fig. 4). Sporangiophores ascendent, 2.5–13 µm diameter, occasionally with long sympodial branches. Sporangia globose, 19–39 × 21–42 µm, dark gray or yellowish-brown sporangia. Columellae globose to subglobose (8.5–14 × 7.5–16.5 µm), with distinct collar. Sporangiospores are smooth, mostly ellipsoidal or subglobose, 2-3 × 2.5-5 µm, usually with granules at each end. Main and lateral hyphae with yellow pigments, occasionally with irregularly spaced septa, usually containing numerous yellowish droplets. Zygospores were not observed. Sporangia on potato dextrose agar (PDA) were smaller (13.5–34 × 14–35 µm diameter) than those on SGA and malt extract agar (MEA) and (17–45 × 16.5–43 µm diameter). The columellae on PDA (6–19.5 × 4.5–21.5 µm) and on MEA (11–23 × 11–23.5 µm) were larger than those on SGA. The shape and size of sporangiospores on SGA, MEA, and PDA were similar. On PDA, arthroconidia and irregularly spaced mycelia are abundant.

Colony characteristics: At 25°C, colonies reach a diameter of 61–63 mm on MEA, 42–63 mm on SDA, and 70–72 mm on SGA after 4 days. At 30°C, colonies reach a diameter of 84–90 mm on SGA, 70–72 mm on MEA, and 45–47 mm on PDA after 4 days. At 37°C,

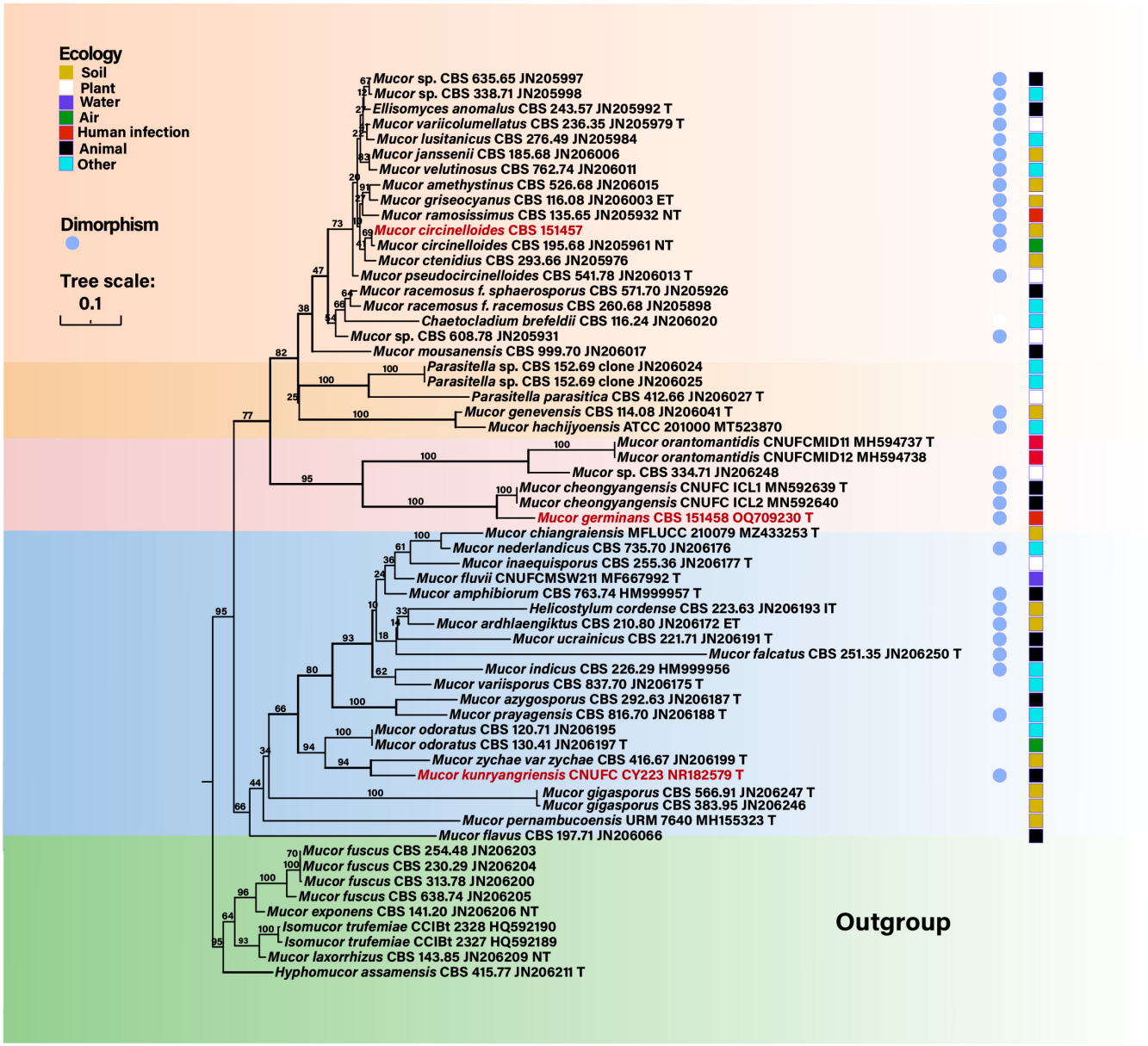

FIG 3 Phylogenetic tree constructed by maximum likelihood algorithm based on rDNA ITS. Bootstrap values are shown with the branches. The three species included in this study are marked in red. Nine mucoralean strains were selected as the outgroups. Blue dots represent the reported dimorphic mucoralean species (31). The squares indicate the ecological position of these strains.

colonies reach a diameter of 40–46 mm on SGA, 33–36 mm on MEA, and 25–26 mm on PDA, after 4 days with no sporulation. Slow growth was observed at temperatures above 40°C.

Notably, *M. germinans* is phylogenetically related to *M. cheongyangensis*. *Mucor germinans* differs from *M. cheongyangensis* by producing smaller sporangia, columellae, and sporangiospores. In addition, *M. germinans* can grow at 37°C, while *M. cheongyangensis* is unable to grow at this temperature.

Antifungal susceptibility

No clinical breakpoints are currently available for any species of *Mucor*. The MIC/MEC (µg/µL) for *M. germinans* were as follows in increasing order: amphotericin B, 0.25 µg/mL;

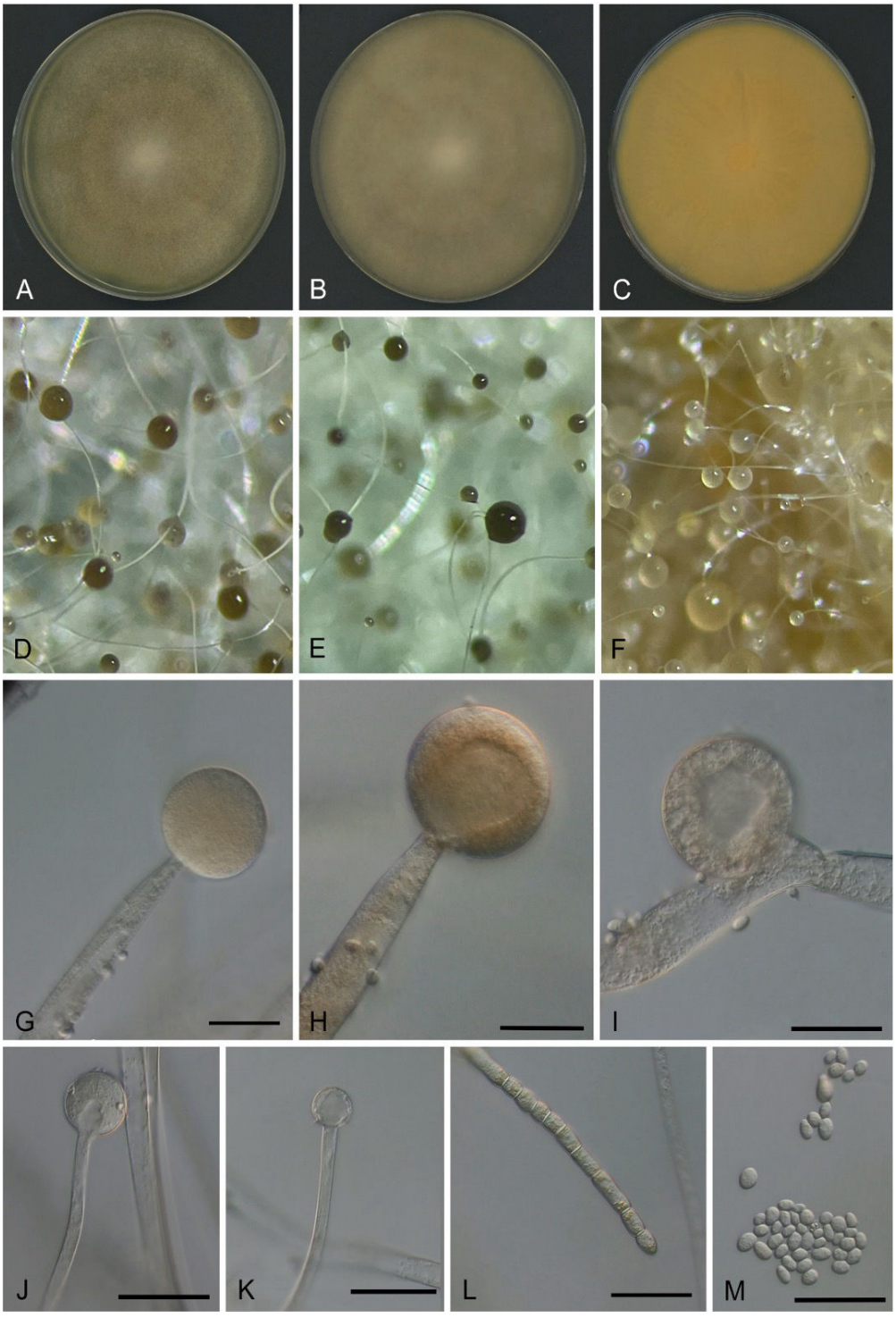

FIG 4 Morphology of *Mucor germinans* on SGA. (A) Colony after 4 days. (B) Colony after 6 days. (C) Colony reverse after 6 days. (D–F) Stereo microscopy of immature and mature sporangia. (G–J) Immature and mature sporangia. (K) Columella after the release of spores. (L) Chlamydospores. (M) Sporangiospores. Scale bars = 20 µm

posaconazole, 0.5 µg/mL; itraconazole, 1 µg/mL; isavuconazole, 8 µg/mL; voriconazole, 16 µg/mL; and micafungin and terbinafine, >16 µg/mL. Table S2 compares the *in vitro* antifungal susceptibility results of *M. germinans* (CBS 151458) with *M. circinelloides* (CBS 151457) and *M. kunryangriensis* (CNUFC CY223). Overall, amphotericin B showed the

lowest minimum inhibitory concentration (MIC) values among antifungals tested against all three *Mucor* strains tested, followed by posaconazole and itraconazole. Isavuconazole showed relatively high MIC/minimum effective concentration (MEC) (≥8 µg/mL) against all strains tested. Consistent with previous reports, our study also showed that voriconazole, micafungin, and terbinafine were not active against three *Mucor* species.

Dimorphism of clinical and environmental strains

Mucor germinans exhibited significantly different morphology when cultured at 25°C or 37°C in shaken liquid culture (Fig. 5). At 25°C in shaken RPMI 1640 without glucose, the spores swelled during the first 3–6 h of incubation. Most of the swollen cells produced germ tubes to form long hyphae with several branches, but some directly converted to yeast-like cells (Fig. 5, left panel). The long hyphae entangled to form round mycelial pellets within 12–24 h (data not shown). Subsequently, some septa appeared at the tips or branches of the mycelium, dividing the mycelium into several compartments (Fig. 5, left panel) and becoming densely septate, giving rise to arthrospores (Fig. 5, left panel). After liberation, arthrospores transformed into yeast-like cells, which produced buds on the surface. In addition, some spherical or fusiform buds were also observed on the surface of intact hyphae.

In shaken RPMI 1640 containing an additional 2% glucose, the production of arthrospores and yeast-like cells increased (Fig. 5, left panel). With 4% additional glucose, yeast cells were preponderant after 72 h of incubation (Fig. 5, left panel).

In RPMI 1640 at 37°C without glucose, buds initiated frequently on the surface of seeded sporangiospores, having yeast-like appearance (Fig. 5, right panel). With extended incubation time, the matured buds were detached and produced new buds, while the subtending cells developed into short, septate hyphal elements. Part of the hyphal elements disarticulated into arthrospores (Fig. 5, right panel). The mother cells finally died. Short hyphae appeared occasionally (Fig. 5, right panel). In RPMI 1640 with 2% and 4% glucose, the production of yeast-like cells increased, eventually with short pseudohyphae (Fig. 5, right panel).

The dimorphic characteristics of *M. circinelloides* were different from those of *M. germinans*. At 25°C in shaken RPMI 1640 with or without glucose, isotropic growth was initially observed during the first 3 h. After 4–6 h, germ tubes were formed, which grew out with numerous filaments that, after 12 h, became entangled, leading to dense pellets. The apical portions of external hyphae of the pellets became densely septate, locally producing clavate daughter cells (Fig. S2, left panel). In part, compartments detached from the hyphae as arthrospores and rounded off and produced yeast-like daughter cells after 72 h of incubation (Fig. S2, left panel). In RPMI 1640 medium without glucose, many chlamydospores appeared (Fig. S2, left panel), with a few arthrospores. At 37°C in shaken media, initially most of the spores of *M. circinelloides* inflated. Some of these cells produced daughter cells, but most of them died. No filamentous form was observed (Fig. S2, right panel).

At 25°C, when shaken in all three media, the seeded sporangiospores of *M. kunryangriensis* initially inflated to spherical cells. Subsequently, a portion of swollen cells produced small budding cells on the surface, while others formed germ tubes. The germ tubes produced several septa to form arthrospores, which produced buds on the surface or separated to form yeast-like cells (Fig. S3, left panel). After 72 h of incubation, budding cells were preponderant, while arthrospores were observed in RPMI 1640 without glucose. Occasionally, short hyphae were formed in RPMI 1640 with 2% glucose. In RPMI 1640 with 4% glucose, yeast-like cells were predominant. When cultured at 37°C in RPMI 1640 with 2% glucose and 4% glucose, swollen cells produced few buds or short germ tubes, while the remainder ruptured and died (Fig. S3, right panel). However, many budding and non-budding yeast-like cells were present in RPMI 1640 without glucose, with occasional dying cells (Fig. S3, right panel).

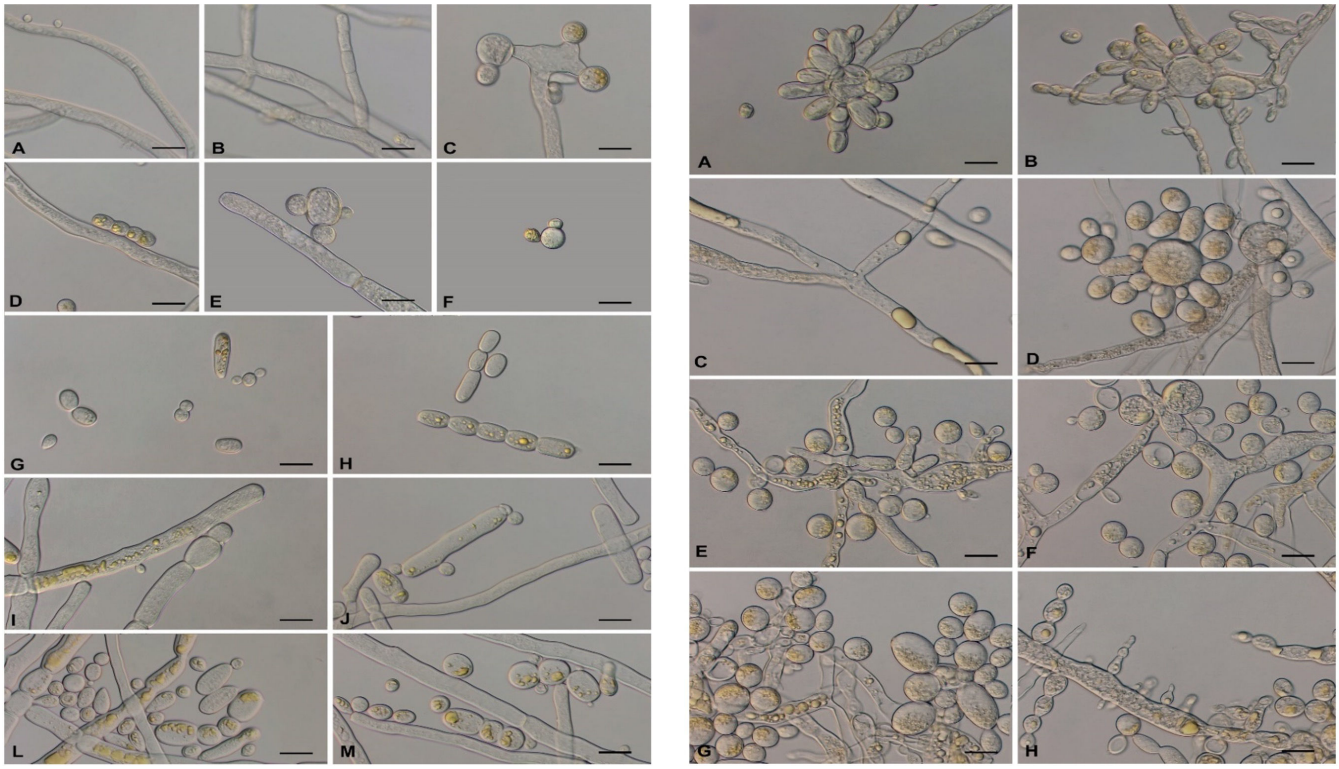

FIG 5 The characteristics of dimorphism in *Mucor germinans* at 25°C (left) and 37°C (right). Left panel: (A–F) the process of filamentous to arthrospores to yeast-like cells cultured at 25°C in RPMI 1640 without glucose. (A and C) Hyphae and budding hyphae. (B) Formation of septate hyphae. (D) Arthrospores. (E and F) Budding yeast-like cells. (G and H) Many yeast-like cells and arthrospores in RPMI 1640 with 2% glucose. (I–M) Yeast-like cells and arthrospores in RPMI 1640 with 4% glucose. Right panel: (A–D) *Mucor germinans* in RPMI 1640 without glucose. (A and B) The budding germ tubes. (C) Occasionally produced long hyphae. (D) Budding yeast-like cells. (E and F) Budding yeast cell formation in RPMI 1640 with 2% glucose. (G and H) Many budding yeast cells and pseudohyphal formation in RPMI 1640 with 4% glucose. Scale bars = 10 µm.

Nuclear staining

Using Hoechst 33258 nucleic acid stain, the cells of *M. germinans* and *M. circinelloides* at 25°C invariably contained multiple nuclei, whether in the form of mycelium, septate hyphae, arthrospores, or yeast cells. In the filamentous form, the nuclei were irregularly distributed throughout the hypha. Upon subdivision of the hyphae into compartments, each cell contained more than three nuclei. With the maturation of the arthrospores, the number of nuclei gradually increased, becoming densely crowded. These multinucleate arthrospores detached from the hyphae and produced new buds. At 37°C, *M. germinans* grew very fast and predominantly survived in the form of budding cells and arthrospores, both of which contained more than six nuclei (Fig. 6). However, the number of nuclei in *M. circinelloides* cells remained significantly lower, and cells had a shorter life span (Fig. S4).

At 25°C, yeast cells of *M. kunryangriensis* initially contained three to six nuclei. Cells inflated and produced buds, and the number of nuclei increased. Daughter cells contained one to three nuclei. After detachment, the number of nuclei increased further. At 37°C, budding cells all had multiple nuclei, even though many cells died in RPMI 1640 with 2% and 4% glucose (Fig. S5).

DISCUSSION

Ruderal strategy of *Mucorales*

Mucorales are unique among the pathogenic fungi in their acute course of infection, whereas nearly all members of closely related fungi in the order *Entomophthorales* result

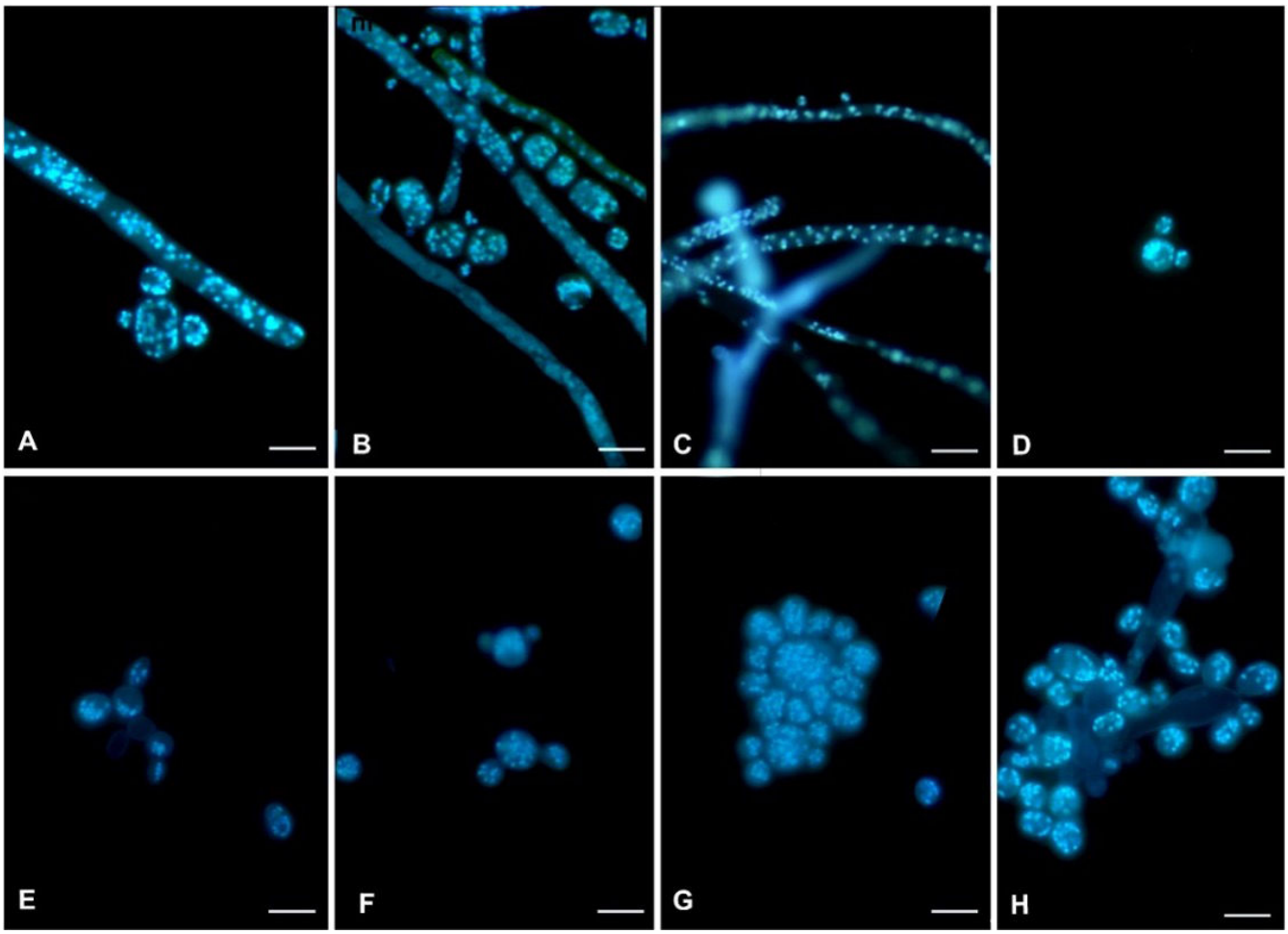

FIG 6 *Mucor germinans* multi-nucleate cells at 25°C and 37°C after fluorescent Hoechst 33258 staining. (A–D). *Mucor germinans* at 25°C. (A, B, and D) Arthrospores and yeast-like cells. (C) Hyphae. (E–H) *Mucor germinans* at 37°C. (E–G) Budding yeast cells. (H) Coherent budding cells. Scale bars = 10 µm.

in chronic infections. This is most likely due to the behavior of *Mucorales* fungi in their natural habitat. They are considered as "microbial weeds" because of their rapid colonization of virgin substrates, which have not yet been occupied by other, competing microbes (33). Various members of *Mucorales* inhabit Asian fermented foods and are widely used in industrial fermentation processes of soy-based foodstuffs (34). Accordingly, it may be hypothesized that their competitive ability is low; they sporulate heavily and die within days, prior to substrate degradation by later-arriving microbes. As a consequence of this strategy, infections in the human patient are aggressive and rapidly deteriorating (35). For their colonization of soft and (semi-)liquid substrates, the ability to produce yeast is beneficial. Decreased sub-surface oxygen and increased carbon dioxide tension are known parameters of mold-to-yeast transition (20, 22, 28, 36).

Dimorphism in *Mucor*

It is unclear, however, why the dimorphic property is more common in *Mucor* species than other *Mucorales* (31). *Rhizopus arrhizus*, *Rhizopus microsporus,* and *Rhizomucor pusillus* proved to be tolerant toward osmotic, oxidative, pH, and metal ion stress, while *Mucor* was more susceptible (37). This suggests a different ecological mainstay in *Mucor*, where unicellularity seems to be more important.

The Cell wall composition of hyphae and budding cells in a *Mucor* strain that was designated as "*Mucor rouxii*" but probably belonged to *Mucor circinelloides* are similar, but the fine structure and thickness are significantly different; the cell wall of yeast

cells has two layers, while the mycelial cells have only a single layer (38). In addition, the cell wall of yeast cells is around 10 times thicker than that of the filamentous form (38). Membranes are strengthened by decreased permeability and increasing cell stiffness (28). Hence, compared with the mycelial morphology, the yeast cells are more stress-tolerant and designed to prevent the leakage of intracellular contents. It may be hypothesized that *Mucor* species are adapted to submersion, low oxygen, and high temperature with yeast-like cells as a protective survival mechanism.

In the present study, we determined three factors that stimulate yeast conversion: temperature, oxygen, and hexose (glucose). Arthrospores acted as an important intermediate to produce yeast-like cells. The production of arthrospores has been hypothesized to be a survival mechanism because it is formed after the cessation of logarithmic growth or under unfavorable nutritional conditions (22). However, excess glucose also stimulates conversion, suggesting ecological similarity with the presence inside nutrient-rich fruit or foodstuffs. Arthrospores occurred in a random manner at the terminal and internal regions of the hyphae (30). Arthrospores were formed in submerged cultures through the septation of normally coenocytic hyphae and the deposition of a new three-layered wall beneath and distinct from the original hyphal wall (19). This septate chain ultimately fragments, releasing spherical cells, which superficially resemble the subsequent budding daughter cells.

Differences are noted between *Mucor* species. The formation of arthrospores was not always the intermediate form for yeast cell production. *M. kunryangriensis* produced daughter cells via budding directly in RPMI 1640 without glucose at 37°C and few arthrospores were observed, while *M. circinelloides* showed preponderantly mycelium-arthrospore-yeast conversion. Arthrospores were also significant in *M. germinans*. However, in general, the morphological dimorphism of *M. circinelloides*, *M. kunryangriensis,* and *M. germinans* is different and is affected by various factors. In this study, their morphological process is summarized in Fig. 7. The differences between *M. circinelloides*, *M. kunryangriensis,* and *M. germinans* matched with their phylogenetic position based on ribosomal DNA (rDNA) ITS (Fig. 3).

Dimorphism is an important morphological characteristic in some filamentous fungi, when associated with host infection in plant or animal pathogenicity (39). Factors stimulating dimorphism vary between species and are closely associated with their habitat. *Candida albicans* (40), *Talaromyces marneffei* (41), and *Paracoccidioides brasiliensis* (24) are known dimorphic pathogens, where, particularly, temperature is a decisive virulence factor that induces morphological change. The plant pathogenic fungus *Zymoseptoria tritici* integrated light, temperature, and plant cues to initiate dimorphism and pathogenesis (42). *Umbilicaria muhlenbergii* is equipped with a variety of physiological and biochemical features that enable survival under stress conditions induced by the presence of heavy metals (43). Nutrient limitation and hyperosmotic stress triggered the dimorphic change in *U. muhlenbergii*, while contact with algal cells of its photobiont *Trebouxia jamesii* induced pseudohyphal growth (44). Overall, the transformation of filamentous fungi into yeast forms is a positive strategy for many fungi adapting to different environments.

Budding in the human host

The potential occurrence of mucoralean budding cells in human tissue has rarely been mentioned in the literature and remains unclear. Among the mucoralean fungi causing disease, *Cokeromyces recurvatus* was the most frequently reported species, existing with yeast cells with mariner's wheel appearance in the vagina of pregnant and non-pregnant women (16, 17, 45–48) and in patients with gastric outlet obstruction (49), pneumonia (50), chronic cystitis (51), and bone marrow transplant (52). *Rhizopus arrhizus* was reported to show abundant yeast-like cells besides the typical mucoralean hyphae in resected bone and soft tissue specimens from a case of sinonasal and palatal mucormycosis (15). Walther (31) plotted yeast conversion abilities on a phylogenetic tree of the *Mucorales* and noted that transformation from hyphae to yeast cells was common,

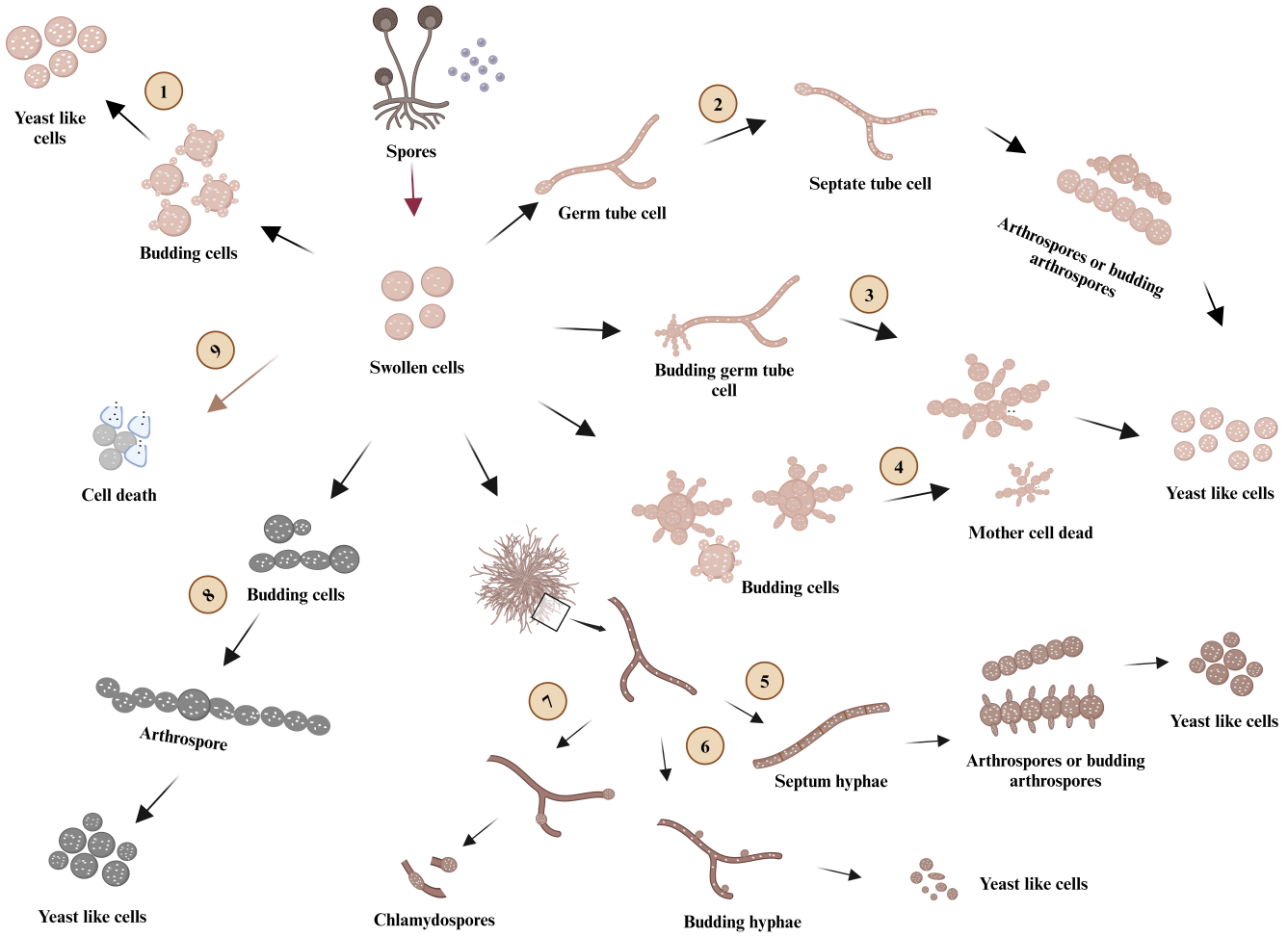

FIG 7 Dimorphism characteristics of three *Mucor* species in RPMI 1640. *Mucor germinans* mainly followed route 1, route 5, and route 6 to form yeast-like cells at 25°C. When cultured at 37°C, *Mucor germinans* produced many yeast-like cells by following routes 3 and 4. At 25°C, *Mucor circinelloides* produced a limited number of yeast-like cells by following route 5 and formed chlamydospores in route 7. Most of the seeding spores of *Mucor circinelloides* grew into swollen cells and finally died (route 9) at 37°C. *Mucor kunryangriensis* produced many yeast-like cells by following route 1, route 2, and route 8 at 25°C, and most of *Mucor kunryangriensis* cells died when cultured at 37°C (route 9). The figure was created using Bio Render (agreement number: HT26YBOGAY, https://app.biorender.com/).

especially in the genus *Mucor*. The criterion for dimorphism was based on induction *in vitro* under high glucose or hypoxia conditions. This evidence demonstrated that dimorphism was widespread and thus could be expected in numerous cases of mucoralean infections in humans. Nevertheless, in the clinical diagnosis of mucormycosis, the possibility of *Mucorales* exhibiting yeast cells has not been perceived.

Infections by members of *Mucorales* are typically rapidly progressive and have a high mortality rate. Severe *Mucorales* infections occur among immunocompromised patients, particularly those with uncontrolled diabetes, hematological malignancy, solid organ transplantation, iron overload, neutropenia, and long-term glucocorticoid use (53). Rhino-orbital, rhino-orbital-cerebral, rhino-cerebral, pulmonary, and cutaneous mucormycosis are the prevalent manifestations of mucormycosis, depending on the comorbidities of the patients. In rhino-orbital and pulmonary mucormycosis associated with COVID-19, uncontrolled diabetes overshadowed all other risk factors (3). COVID-associated renal, gastrointestinal (53), small bowel (54), and esophageal mucormycosis (55) have also been reported. Especially during the second wave of the COVID-19 pandemic, devastating cases of COVID-19-associated mucormycosis were observed

worldwide, with a mortality rate of up to 80% (3, 53). The hyphae tend to occlude blood vessels (35), leading to necrosis of efferent tissues and causing impressive clinical appearance. If no therapy is applied, the disease is potentially fatal. Susceptibility to some of the commonly applied antifungals differs between species, which necessitates rapid and accurate species identification (53). Given the acute nature of mucoralean infections, rapid identification of the culprit is imperative for beneficial clinical outcomes.

Recognition of mucoralean yeast in the patient

Direct microscopic visualization of non-septate hyphae by fluorescent dyes and culture are the cornerstones of diagnosis but are insufficient to reach species identity (1). The budding cells of *Mucor germinans* in this study and in the previous reports of *Cokeromyces recurvatus* were highly similar to those of *Paracoccidioides* species in direct microscopic examination. Budding in *Candida* and *Cryptococcus* is subterminal or monopolar, respectively, and buds never appear over the entire surface of the mother cells. It is possible that the yeast cells of *Mucorales* are misidentified as any of these fungi. The anamnesis of the patient usually excludes paracoccidioidomycosis, which is a systemic mycosis endemic to South America (56). Otherwise, the nuclear condition of mucoralean cells is a useful diagnostic tool. Mucoralean yeast cells are invariably multi-nucleate at 25°C as well as at 37°C; this feature might be used for rapid clinical diagnostics. Budding cells of *Candida* and *Cryptococcus* are mononuclear (57). *Paracoccidioides* may be problematic because its yeast cells are initially mononuclear but become multinucleated after inflation (58). The potential misconception of a fungus having a chronic course of infection may lead to a significant delay in identification and treatment.

Therapeutic consequences

Antifungal susceptibility in *Mucorales* shows differences between genera (33, 59). Therefore, it is important for mucormycosis to identify the species level of the pathogen as quickly as possible to improve clinical management. *Mucor* species are usually sensitive to amphotericin B but show often higher MICs to isavuconazole, itraconazole, and posaconazole than species of *Rhizopus* and *Lichtheimia* spp. (53). In the present case, the patient received posaconazole infusion as prophylaxis, and amphotericin B was not added to the treatment regimen until the *Mucor* species was isolated from the sputum sample. *In vitro* antifungal testing of *M. germinans* showed that it was sensitive to amphotericin B with a low MIC and was resistant to azoles. This case report highlights the importance of species-level identification in mucoralean infection. Importantly, although *Mucorales* are usually taken to be strictly filamentous, they may occasionally manifest yeast-like cells in patients. This phenomenon may mislead clinical diagnosis and appropriate treatment for mucormycosis. As a result, it is necessary to investigate the dimorphic properties of *Mucorales* for a better understanding of its clinical significance of dimorphism in mucormycosis and to improve therapeutic approaches for mucormycosis.

MATERIALS AND METHODS

Strains analyzed

The strain described in this study was derived from human sputum at the Department of Laboratory Medicine, National Institutes of Health Clinical Center in Bethesda, MD, USA, preserved as SM1517 (CBS 151458). Comparative analysis of yeast phases was performed with a strain of *M. circinelloides* isolated from compost obtained from a flower store in Rotterdam, The Netherlands, maintained at Radboud University, Nijmegen under No. 22240565201 (CBS 151457), and with the strain of *M. kunryangriensis*, originally isolated from the body of a cricket insect (*Gryllus* sp.) in South Korea (60), preserved as CNUFC CY223 at the Environmental Microbiology Laboratory Fungarium, Chonnam National University, Gwangju, South Korea.

Morphology

Pure cultures of *M. germinans* were cultured on potato dextrose agar (PDA, Loifichem, Abruzzi, Italy), malt extract agar (MEA, VWR Chemicals, Netherlands), and Sabouraud glucose agar (Sigma-Aldrich, Darmstadt, Germany). The plates were incubated at 30°C for 5 days. Fragments of mycelia were isolated from the cultures and placed onto microscopy slides with Shear's fluid. Carl Zeiss microscope GmbH 37081 (Carl Zeiss, Germany) possessing differential interference contrast optics was used to obtain digital images.

Culture conditions and physiology

Cardinal growth temperatures of *M. germinans* were determined on PDA, MEA, and SGA. Plates were incubated in the dark for 5 days at temperatures of 25°C, 30°C, 37°C, 40°C, and 45°C, with three simultaneous replicates for each isolate. Colony expansion was measured daily. Spores of *M. germinans*, *M. circinelloides,* and *M. kunryangriensis* grown on SGA at 28°C for 3 days were harvested with a sterile cotton swab, suspended in sterile demi-water, and adjusted to 1×10^6 spores/mL using Neubauer's cell count chambers. A volume of 500 µL of spore suspension was added to culture flasks with 20 mL RPMI 1640 media containing RPMI 1640 (Biowest, USA, 20.8 g/L) and MOPS (morpholinepropanesulfonic acid; Sigma-Aldrich, Darmstadt, Germany, 69.06 g/L). In addition, 10 N NaOH (Sigma-Aldrich, Darmstadt, Germany) was added to maintain the pH at 7.0. D-Glucose (Sigma-Aldrich, Darmstadt, Germany) was added to maintain the glucose concentration at 2% and 4%, respectively. The final spore density of culture was 2.5×10^4 spores/mL, and flasks were incubated at 25°C and 37°C on a shaking incubator at 170 r.p.m. for 72 h, as described previously (61).

Fluorescence microscopy

Dimorphism of the *M. germinans*, *M. circinelloides,* and *M. kunryangriensis* was monitored on a daily basis using fluorescence microscopy. Strains were transferred to sterile tubes containing 500 mL phosphate-buffered saline (PBS), shaken for 10 s, centrifuged for 3 min at 3,000 r.p.m., and washed twice with 500 µL of PBS. After the removal of PBS, samples were subjected to a series of 100 µL alcohol of 50%, 80%, and 96% and centrifuged for 3 min at 3,000 r.p.m, shaken for 10 s, and incubated for 3 min at 25°C. After removing alcohol, samples were allowed to dry before 100 µL of 1 µg/mL Hoechst 33258 (Sigma-Aldrich, Darmstadt, Germany) was added, shaken for 10 s, and incubated in the dark for 5 min prior to fluorescence microscopy (62).

DNA extraction of fungal strains, amplification, and sequencing

Mucor isolates were grown on SGA for 3 days at 28°C, and the sporangiophores were picked to extract DNA using the rapid DNA extraction method as previously described with some modifications (63). Sporangiospores were added into sterilized tubes with 250 µL breaking buffer and glass beads (425–600 diameter). Samples were shaken at 1,500 r.p.m. for 30 min at 70°C. Subsequently, 200 µL phenol-chloroform-isoamyl alcohol (25:24:1, Sigma, USA) was added, and the mixture was centrifuged at 13,000 r.p.m. for 15 min at room temperature to collect the upper phase for PCR amplification. Primers ITS 1 and ITS 4 were used to amplify the ITS rDNA region (63). Gel Purification Kit (QIAquick, Hilden, Germany) was applied for PCR product purification. Automated sequencing was performed with the same primers based on Sanger sequencing.

Alignment and phylogenetic reconstruction

The resulting DNA sequences were checked and assembled via SeqMan in the Lasergene package. The newly generated sequences were blasted in NCBI GenBank and MycoBank databases. Sequences were submitted to the GenBank database under the accession numbers provided in Table S1. Sequence data of closely related *Mucor* spp. were selected from the data previously published (21, 31, 60, 64–67) and downloaded from GenBank

(accessed on 11 September 2023) for the construction of molecular phylogeny (Table S1). ITS sequences (60 taxa) were aligned using MAFFT (http://mafft.cbrc.jp/, accessed on 12 September 2023) with the algorithm LINS-I, and the alignment results were checked and trimmed in Bioedit v7.0.5.3. Data were converted from Fasta format to Phylip format using the CIPRES portal (http://www.phylo.org; accessed 13 September 2023). Phylogenetic reconstructions were carried out by maximum likelihood (ML) using RAxML-HPC BlackBox. We performed the ML analysis using 1,000 bootstrap replicates under the best substitution model for the ITS (TPM2uf + I + G). The resulting trees were viewed using FigTree v1.4.4 (http://tree.bio.ed.ac.uk/software/figtree/) and modified via iTols.

MALDI-ToF MS

The matrix-assisted laser desorption/ionization time-of-flight mass spectrometry (MALDI Biotyper Bruker Daltonics Inc., Billerica, MA, USA) was used for the identification of the clinical strain. Fungal material (approximately the size of a small pencil eraser) was taken using a sterile culture swab and added to a tube containing 70% ethanol and silica beads. Using a high-speed tissue homogenizer (MO BIO PowerLyser instrument, Qiagen, USA), the fungal cell was lysed for 30 s and 4,000 r.p.m. From the lysed cells, proteins were released into the supernatant of the solvent mixture. This supernatant was used to inoculate a microtiter plate on the MALDI-ToF MS instrument.

Direct PCR sequencing of sputum sample

Nucleic acid extraction was performed on the sputum sample by the use of an automated EZ1 extraction instrument (Qiagen, Germany), according to the manufacturer's recommendations, followed by PCR sequencing of the ITS region of rDNA. The resulting DNA sequences were aligned to both the NCBI GenBank (http://www.ncbi.nlm.nih.gov/genbank) and the International Mycological Association-Westerdijk Fungal Biodiversity Institute (http://www.mycobank.org) databases.

Antifungal susceptibility

Antifungal susceptibility testing for amphotericin B, itraconazole, isavuconazole, micafungin, posaconazole, terbinafine, and voriconazole was performed by broth microdilution according to the Clinical and Laboratory Standards Institute (CLSI) standard CLSI M38-A3 guidelines. Stock solutions of each drug were prepared by dissolving the powders in dimethyl sulfoxide, and further dilutions were prepared in RPMI buffered with 0.165 M MOPS (pH 7.0) and 0.2% glucose, without bicarbonate and with phenol red, with the final concentrations for each antifungal ranging from 0.016 to 16 mg/mL. Minimum inhibitory concentrations were read visually at 100% inhibition of growth after 24 h of incubation at 35°C for tested drugs. The MIC was defined as the lowest concentration that completely inhibited growth as assessed by visual inspection in comparison with the control (drug-free well). For micafungin, the MEC was defined as the lowest concentration in which abnormal, short, and branched hyphal clusters were observed, in contrast to the long, unbranched hyphal elements that were seen in the well. *Candida parapsilosis* (ATCC 22019) and *Candida krusei* (ATCC 6258) were used for quality controls in all experiments. All experiments on each strain were performed using three independent replicates on different days.

ACKNOWLEDGMENTS

The work of N.L. was supported by China Scholarship Council (No.202108520042). Y.K. was supported by 111 Project (D20009), China-Ukraine Intergovernmental Exchange Project (8), National Natural Science Foundation of China (NSFC, No. 32060034), International Science and Technology Cooperation Base of Guizhou Province [(2020)4101], Talent Base Project of Guizhou Province (RCJD2018-22), High-level Innovation Talent Project of Guizhou Province [GCC(2022)036-1], Major Science and

Technology Projects of China Tobacco [No.110202101048 (LS-08)], Foundation of Key Laboratory of Microbiology and Parasitology of Education Department of Guizhou [QJJ (2022) 019], Ministry of Education Project (07150120711), China. H.B.L. was supported by a research grant (2022M3H9A1082984) from the Ministry of Science and ICT and (2022R1I1A3068645) from the Ministry of Education, National Research Foundation of Korea. J.C.-R. and K.J.K.-C. were supported by a research fund from the intramural program of the National Institute of Allergy and Infectious Diseases, National Institutes of Health, Bethesda, MD, USA. C.K. is supported by the Intramural Research Program of the National Cancer Institute, National Institutes of Health (NIH), and the Lasker Foundation. A.S. was supported by a research fund (Project ID: ZIA CL090088) from the intramural research program of the National Institutes of Health, Clinical Center, Bethesda, MD, USA.

AUTHOR AFFILIATIONS

[1]Key Laboratory of Environmental Pollution Monitoring and Disease Control, Ministry of Education of Guizhou, Guizhou Medical University, Guiyang, China
[2]Key Laboratory of Medical Microbiology and Parasitology, School of Basic Medical Sciences, Guizhou Medical University, Guiyang, China
[3]RadboudUMC-CWZ Center for Expertise in Mycology, Nijmegen, the Netherlands
[4]Microbiology Service, Department of Laboratory Medicine, Clinical Center, National Institutes of Health, Bethesda, Maryland, USA
[5]Laboratory of Clinical Immunology and Microbiology, National Institute of Allergy and Infectious Diseases, National Institutes of Health, Bethesda, Maryland, USA
[6]Center for Immuno-Oncology, Center for Cancer Research, National Cancer Institute, National Institutes of Health, Bethesda, Maryland, USA
[7]Laboratory of Pathology, National Cancer Institute, National Institutes of Health, Bethesda, Maryland, USA
[8]Natural and Medical Sciences Research Centre, University of Nizwa, Nizwa, Oman
[9]Department of Pathobiology, Ontario Veterinary College, University of Guelph, Guelph, Ontario, Canada
[10]Vet Veterinary Diagnostic Laboratory, Tehran, Iran
[11]German National Reference Center for Invasive Fungal Infections, Leibniz Institute for Natural Product Research and Infection Biology, Hans Knöll Institute, Jena, Germany
[12]Institution of One Health Research, Guizhou Medical University, Guiyang, China.
[13]Environmental Microbiology Laboratory, Department of Agricultural Biological Chemistry, College of Agriculture and Life Sciences, Chonnam National University, Gwangju, South Korea

AUTHOR ORCIDs

Na Li http://orcid.org/0000-0002-4713-0705
Sybren de Hoog http://orcid.org/0000-0002-5344-257X
Christopher G. Kanakry http://orcid.org/0000-0002-7736-2056
Sarah A. Ahmed http://orcid.org/0000-0003-0155-8113
Abdullah M. S. Al-Hatmi http://orcid.org/0000-0002-5206-2647
Kyung J. Kwon-Chung http://orcid.org/0000-0001-6671-0994
Yingqian Kang http://orcid.org/0009-0005-6033-447X
Hyang Burm Lee http://orcid.org/0000-0001-5353-2586
Amir Seyedmousavi http://orcid.org/0000-0002-6194-7447

FUNDING

Funder	Grant(s)	Author(s)
HHS | National Institutes of Health (NIH)	ZIA CL090088	Amir Seyedmousavi

AUTHOR CONTRIBUTIONS

Na Li, Data curation, Methodology, Software, Writing – original draft | Jennifer Bowling, Data curation, Methodology, Software, Writing – original draft | Sybren de Hoog, Formal analysis, Investigation, Project administration, Resources, Supervision, Validation, Writing – original draft, Writing – review and editing | Chioma I. Aneke, Methodology | Jung-Ho Youn, Methodology | Sherin Shahegh, Methodology | Jennifer Cuellar-Rodriguez, Investigation, Resources, Writing – review and editing | Christopher G. Kanakry, Investigation, Resources, Writing – review and editing | Maria Rodriguez Pena, Methodology | Sarah A. Ahmed, Software | Abdullah M. S. Al-Hatmi, Software | Ali Tolooe, Investigation, Software, Writing – review and editing | Grit Walther, Formal analysis, Investigation, Software, Writing – review and editing | Kyung J. Kwon-Chung, Conceptualization, Formal analysis, Investigation, Supervision, Writing – review and editing | Yingqian Kang, Funding acquisition, Resources, Writing – review and editing | Hyang Burm Lee, Data curation, Methodology, Resources, Writing – review and editing | Amir Seyedmousavi, Conceptualization, Data curation, Formal analysis, Funding acquisition, Investigation, Methodology, Project administration, Resources, Software, Supervision, Validation, Visualization, Writing – original draft, Writing – review and editing

ADDITIONAL FILES

The following material is available online.

Supplemental Material

Supplemental Figures (mBio00144-24-S0001.pdf). Fig. S1 to S5.
Table S1 (mBio00144-24-s0002.docx). Taxa, collection numbers, and GenBank accession numbers used in this study.

REFERENCES

1. Cornely OA, Alastruey-Izquierdo A, Arenz D, Chen SCA, Dannaoui E, Hochhegger B, Hoenigl M, Jensen HE, Lagrou K, Lewis RE, et al. 2019. Global guideline for the diagnosis and management of mucormycosis: an initiative of the European confederation of medical mycology in cooperation with the mycoses study group education and research consortium. Lancet Infect Dis 19:e405–e421. https://doi.org/10.1016/S1473-3099(19)30312-3
2. Skiada A, Lass-Floerl C, Klimko N, Ibrahim A, Roilides E, Petrikkos G. 2018. Challenges in the diagnosis and treatment of mucormycosis. Med Mycol 56:93–101. https://doi.org/10.1093/mmy/myx101
3. Muthu V, Agarwal R, Patel A, Kathirvel S, Abraham OC, Aggarwal AN, Bal A, Bhalla AS, Chhajed PN, Chaudhry D, et al. 2022. Definition, diagnosis, and management of COVID-19-associated pulmonary mucormycosis: delphi consensus statement from the fungal infection study forum and academy of pulmonary sciences, India. Lancet Infect Dis 22:e240–e253. https://doi.org/10.1016/S1473-3099(22)00124-4
4. Hussain S, Baxi H, Riad A, Klugarová J, Pokorná A, Slezáková S, Líčeník R, Najmi AK, Klugar M. 2021. COVID-19-associated mucormycosis (CAM): an updated evidence mapping. Int J Environ Res Public Health 18:10340. https://doi.org/10.3390/ijerph181910340
5. Patel A, Kaur H, Xess I, Michael JS, Savio J, Rudramurthy S, Singh R, Shastri P, Umabala P, Sardana R, Kindo A, Capoor MR, Mohan S, Muthu V, Agarwal R, Chakrabarti A. 2020. A Multicentre observational study on the epidemiology, risk factors, management and outcomes of Mucormycosis in India. Clin Microbiol Infect 26:944. https://doi.org/10.1016/j.cmi.2019.11.021
6. Skiada A, Pagano L, Groll A, Zimmerli S, Dupont B, Lagrou K, Lass-Florl C, Bouza E, Klimko N, Gaustad P, Richardson M, Hamal P, Akova M, Meis JF, Rodriguez-Tudela J-L, Roilides E, Mitrousia-Ziouva A, Petrikkos G, European Confederation of Medical Mycology Working Group on Zygomycosis. 2011. Zygomycosis in Europe: analysis of 230 cases accrued by the registry of the European confederation of medical mycology (ECMM) working group on zygomycosis between 2005 and 2007. Clin Microbiol Infect 17:1859–1867. https://doi.org/10.1111/j.1469-0691.2010.03456.x
7. Dam P, Cardoso MH, Mandal S, Franco OL, Sağıroğlu P, Polat OA, Kokoglu K, Mondal R, Mandal AK, Ocsoy I. 2023. Surge of mucormycosis during the COVID-19 pandemic. Travel Med Infect Dis 52:102557. https://doi.org/10.1016/j.tmaid.2023.102557
8. Joshi S, Telang R, Tambe M, Havaldar R, Sane M, Shaikh A, Roy C, Yathati K, Sonawale S, Borkar R, Magar R, Bhitkar H, Shitole S, Nakate L, Kudrimoti J, Mave V. 2022. Outbreak of Mucormycosis in Coronavirus disease patients, Pune, India. Emerg Infect Dis 28:1–8. https://doi.org/10.3201/eid2801.211636
9. Darwish RM, AlMasri M, Al-Masri MM. 2022. Mucormycosis: the hidden and forgotten disease. J Appl Microbiol 132:4042–4057. https://doi.org/10.1111/jam.15487
10. Walsh TJ, Gamaletsou MN, McGinnis MR, Hayden RT, Kontoyiannis DP. 2012. Early clinical and laboratory diagnosis of invasive pulmonary, extrapulmonary, and disseminated mucormycosis (zygomycosis). Clin Infect Dis 54 Suppl 1:S55–60. https://doi.org/10.1093/cid/cir868
11. Frater JL, Hall GS, Procop GW. 2001. Histologic features of zygomycosis: emphasis on perineural invasion and fungal morphology. Arch Pathol Lab Med 125:375–378. https://doi.org/10.5858/2001-125-0375-HFOZ
12. Lass-Flörl C. 2009. Zygomycosis: conventional laboratory diagnosis. Clin Microbiol Infect 15 Suppl 5:60–65. https://doi.org/10.1111/j.1469-0691.2009.02999.x
13. Monheit Je Fau - Cowan DF, Cowan Df Fau - Moore DG. 1984. Rapid detection of fungi in tissues using calcofluor white and fluorescence microscopy. Arch Pathol Lab Med 108:616–618.
14. Lass-Flörl Cornelia, Resch G, Nachbaur D, Mayr A, Gastl G, Auberger J, Bialek R, Freund MC. 2007. The value of computed tomography-guided percutaneous lung biopsy for diagnosis of invasive fungal infection in immunocompromised patients. Clin Infect Dis 45:e101–4. https://doi.org/10.1086/521245
15. Kantarcioğlu AS, Yücel A, Nagao K, Sato T, Inci E, Ogreden S, Kaytaz A, Alan S, Bozdağ Z, Edali N, Sar M, Kepil N, Oz B, Altas K. 2006. A *Rhizopus*

oryzae strain isolated from resected bone and soft tissue specimens from a sinonasal and palatal mucormycosis case. Report of a case and *in vitro* experiments of yeast-like cell development. Med Mycol 44:515–521. https://doi.org/10.1080/13693780600764973
16. Khaitan N, Booth CN, Hoda RS. 2021. *Cokeromyces recurvatus*: a rare fungus in the Pap test of an asymptomatic woman. Diagn Cytopathol 49:894–895. https://doi.org/10.1002/dc.24758
17. Paquette C, Slater SE, McMahon MD, Quddus MR. 2016. *Cokeromyces recurvatus* in a cervical papanicolaou test: a case report of a rare fungus with a brief review of the literature. Diagn Cytopathol 44:419–421. https://doi.org/10.1002/dc.23432
18. Díaz-Pérez SP, Patiño-Medina JA, Valle-Maldonado MI, López-Torres A, Jácome-Galarza IE, Anaya-Martínez V, Gómez-Ruiz V, Campos-García J, Nuñez-Anita RE, Ortiz-Alvarado R, Ramírez-Díaz MI, Gutiérrez-Corona JF, Meza-Carmen V. 2020. Alteration of fermentative metabolism enhances *Mucor circinelloides* virulence. Infect Immun 88:e00434–00419. https://doi.org/10.1128/IAI.00434-19
19. Barrera CR. 1983. Formation and ultrastructure of *Mucor rouxii* arthrospores. J Bacteriol 155:886–895. https://doi.org/10.1128/jb.155.2.886-895.1983
20. Bartnicki-Garcia S, NICKERSON WJ. 1962. Induction of yeast-like development in *Mucor* by carbon dioxide. J Bacteriol 84:829–840. https://doi.org/10.1128/jb.84.4.829-840.1962
21. Wagner L, Stielow JB, de Hoog GS, Bensch K, Schwartze VU, Voigt K, Alastruey-Izquierdo A, Kurzai O, Walther G. 2020. A new species concept for the clinically relevant *Mucor circinelloides* complex. Persoonia 44:67–97. https://doi.org/10.3767/persoonia.2020.44.03
22. Orlowski M. 1991. *Mucor* dimorphism. Microbiol Rev 55:234–258. https://doi.org/10.1128/mr.55.2.234-258.1991
23. Karmakar M, Ghosh B, Ray RR. 2012. Effect of extracellular factors on growth and dimorphism of *Rhizopus oryzae* with multiple enzyme synthesizing ability. Indian J Microbiol 52:215–221. https://doi.org/10.1007/s12088-011-0197-z
24. Hahn RC, Hagen F, Mendes RP, Burger E, Nery AF, Siqueira NP, Guevara A, Rodrigues AM, de Camargo ZP. 2022. Paracoccidioidomycosis: current status and future trends. Clin Microbiol Rev 35:e0023321. https://doi.org/10.1128/cmr.00233-21
25. Brilhante RSN, Silva MLQ da, Pereira VS, de Oliveira JS, Maciel JM, Silva ING da, Garcia LGS, Guedes GM de M, Cordeiro R de A, Pereira-Neto W de A, de Camargo ZP, Rodrigues AM, Sidrim JJC, Castelo-Branco D de SCM, Rocha MFG. 2019. Potassium iodide and miltefosine inhibit biofilms of *Sporothrix schenckii* species complex in yeast and filamentous forms. Med Mycol 57:764–772. https://doi.org/10.1093/mmy/myy119
26. Lau SKP, Tsang CC, Woo PCY. 2017. *Talaromyces marneffei* genomic, transcriptomic, proteomic and metabolomic studies reveal mechanisms for environmental adaptations and virulence. Toxins (Basel) 9:192. https://doi.org/10.3390/toxins9060192
27. Jiang Y, Dukik K, Muñoz JF, Sigler L, Schwartz IS, Govender NP, Kenyon C, Feng P, van den Ende BG, Stielow JB, Stchigel AM, Lu H, de Hoog S. 2018. Phylogeny, ecology and taxonomy of systemic pathogens and their relatives in ajellomycetaceae (Onygenales): blastomyces, emergomyces, emmonsia, emmonsiellopsis. Fungal Diversity 90:245–291. https://doi.org/10.1007/s13225-018-0403-y
28. Moriwaki-Takano M, Iwakura R, Hoshino K. 2021. Dimorphic mechanism on cAMP mediated signal pathway in *Mucor circinelloides*. Appl Biochem Biotechnol 193:1252–1265. https://doi.org/10.1007/s12010-020-03342-6
29. Patiño-Medina JA, Maldonado-Herrera G, Pérez-Arques C, Alejandre-Castañeda V, Reyes-Mares NY, Valle-Maldonado MI, Campos-García J, Ortiz-Alvarado R, Jácome-Galarza IE, Ramírez-Díaz MI, Garre V, Meza-Carmen V. 2018. Control of morphology and virulence by ADP-ribosylation factors (ARF) in *Mucor circinelloides*. Curr Genet 64:853–869. https://doi.org/10.1007/s00294-017-0798-0
30. Lübbehüsen TL, Nielsen J, McIntyre M. 2003. Characterization of the *Mucor circinelloides* life cycle by on-line image analysis. J Appl Microbiol 95:1152–1160. https://doi.org/10.1046/j.1365-2672.2003.02098.x
31. Walther G. 2023. Molecular phylogeny and character evolution of *Mucorales*. In Westerdijk spring symposium fungal evolution. Amsterdam.
32. Narayanan S, Chua JV, Baddley JW. 2022. Coronavirus disease 2019-associated mucormycosis: risk factors and mechanisms of disease. Clin Infect Dis 74:1279–1283. https://doi.org/10.1093/cid/ciab726
33. de Hoog GS, Guarro J, Gené J, Ahmed SA, Al-Hatmi AMS, Figueras MJ, Vitale RG. 2020. *Atlas of clinical fungi*. 4th ed, p 1599
34. Liu L, Chen X, Hao L, Zhang G, Jin Z, Li C, Yang Y, Rao J, Chen B. 2022. Traditional fermented soybean products: processing, flavor formation, nutritional and biological activities. Crit Rev Food Sci Nutr 62:1971–1989. https://doi.org/10.1080/10408398.2020.1848792
35. Petrikkos G, Skiada A, Lortholary O, Roilides E, Walsh TJ, Kontoyiannis DP. 2012. Epidemiology and clinical manifestations of mucormycosis. Clin Infect Dis 54 Suppl 1:S23–34. https://doi.org/10.1093/cid/cir866
36. Lee SC, Li A, Calo S, Heitman J. 2013. Calcineurin plays key roles in the dimorphic transition and virulence of the human pathogenic zygomycete *Mucor circinelloides*. PLoS Pathog 9:e1003625. https://doi.org/10.1371/journal.ppat.1003625
37. Singh P, Paul S, Shivaprakash MR, Chakrabarti A, Ghosh AK. 2016. Stress response in medically important *Mucorales*. Mycoses 59:628–635. https://doi.org/10.1111/myc.12512
38. BARTNICKI-GARCIA S, NICKERSON WJ. 1962. Isolation, composition, and structure of cell walls of filamentous and yeast-like forms of *Mucor rouxii*. Biochim Biophys Acta 58:102–119. https://doi.org/10.1016/0006-3002(62)90822-3
39. Klein BS, Tebbets B. 2007. Dimorphism and virulence in fungi. Curr Opin Microbiol 10:314–319. https://doi.org/10.1016/j.mib.2007.04.002
40. Honorato L, de Araujo JFD, Ellis CC, Piffer AC, Pereira Y, Frases S, de Sousa Araújo GR, Pontes B, Mendes MT, Pereira MD, Guimarães AJ, da Silva NM, Vargas G, Joffe L, Del Poeta M, Nosanchuk JD, Zamith-Miranda D, Dos Reis FCG, de Oliveira HC, Rodrigues ML, de Toledo Martins S, Alves LR, Almeida IC, Nimrichter L. 2022. Extracellular vesicles regulate biofilm formation and yeast-to-hypha differentiation in *Candida albicans*. mBio 13:e0030122. https://doi.org/10.1128/mbio.00301-22
41. Wang F, Han R, Chen S. 2023. An overlooked and underrated endemic mycosis-talaromycosis and the pathogenic fungus *Talaromyces marneffei*. Clin Microbiol Rev 36:e0005122. https://doi.org/10.1128/cmr.00051-22
42. Kilaru S, Fantozzi E, Cannon S, Schuster M, Chaloner TM, Guiu-Aragones C, Gurr SJ, Steinberg G. 2022. Zymoseptoria tritici white-collar complex integrates light, temperature and plant cues to initiate dimorphism and pathogenesis. Nat Commun 13:5625. https://doi.org/10.1038/s41467-022-33183-2
43. Kolhe N, Damle E, Pradhan A, Zinjarde S. 2022. A comprehensive assessment of *Yarrowia lipolytica* and its interactions with metals: current updates and future prospective. Biotechnol Adv 59:107967. https://doi.org/10.1016/j.biotechadv.2022.107967
44. Wang Y, Wei X, Bian Z, Wei J, Xu JR. 2020. Coregulation of dimorphism and symbiosis by cyclic AMP signaling in the lichenized fungus *Umbilicaria muhlenbergii*. Proc Natl Acad Sci USA 117:23847–23858. https://doi.org/10.1073/pnas.2005109117
45. Kemna ME, Neri RC, Ali R, Salkin IF. 1994. *Cokeromyces recurvatus*, a mucoraceous zygomycete rarely isolated in clinical laboratories. J Clin Microbiol 32:843–845. https://doi.org/10.1128/jcm.32.3.843-845.1994
46. Nielsen C, Sutton DA, Matise I, Kirchhof N, Libal MC. 2005. Isolation of *Cokeromyces recurvatus*, initially misidentified as *Coccidioides immitis*, from peritoneal fluid in a cat with jejunal perforation. J Vet Diagn Invest 17:372–378. https://doi.org/10.1177/104063870501700413
47. Odronic SI, Scheidemantel T, Tuohy MJ, Chute D, Procop GW, Booth CN. 2012. Two cases of *Cokeromyces recurvatus* in liquid-based papanicolaou tests and a review of the literature. Arch Pathol Lab Med 136:1593–1596. https://doi.org/10.5858/arpa.2011-0493-CR
48. Racher ML. 2020. Eradication of *Cokeromyces recurvatus* in a pregnant patient: a case report. Case Rep Womens Health 28:e00254. https://doi.org/10.1016/j.crwh.2020.e00254
49. Wondimu B, Bradley B, Lieberman JA, Cohen S, Bui L, Reddi D. 2022. Cokeromyces Recurvatus incidentally found in a patient with gastric outlet obstruction. Mycopathologia 187:605–610. https://doi.org/10.1007/s11046-022-00654-5
50. Ryan LJ, Ferrieri P, Powell RD Jr, Paddock CD, Zaki SR, Pambuccian SE. 2011. Fatal *Cokeromyces recurvatus* pneumonia: report of a case highlighting the potential for histopathologic misdiagnosis as *Coccidioides*. Int J Surg Pathol 19:373–376. https://doi.org/10.1177/1066896908330483

51. Axelrod P, Kwon-Chung KJ, Frawley P, Rubin H. 1987. Chronic cystitis due to *Cokeromyces recurvatus*: a case report. J Infect Dis 155:1062–1064. https://doi.org/10.1093/infdis/155.5.1062
52. Tsai TW, Hammond LA, Rinaldi M, Martin K, Tio F, Maples J, Freytes CO, Roodman GD. 1997. *Cokeromyces recurvatus* infection in a bone marrow transplant recipient. Bone Marrow Transplant 19:301–302. https://doi.org/10.1038/sj.bmt.1700647
53. Borman AM, Fraser M, Patterson Z, Palmer MD, Johnson EM. 2021. *In vitro* antifungal drug resistance profiles of clinically relevant members of the *Mucorales* (Mucoromycota) especially with the newer triazoles. JoF 7:271. https://doi.org/10.3390/jof7040271
54. Demir L, Calame P. 2023. Small-bowel mucormycosis at dual-energy CT. Radiology 307:e223271. https://doi.org/10.1148/radiol.223271
55. Harikrishnan VS, Niyas VKM, Arjun R, Murlidharan P, Sasidharan M, Aswini Rajeswari R. 2023. Esophageal mucormycosis. QJM 116:547–548. https://doi.org/10.1093/qjmed/hcad031
56. Krakhecke-Teixeira AG, Yamauchi DH, Rossi A, de Sousa HR, Garces HG, Júnior JL, Júnior AOS, Felipe MSS, Bagagli E, de Andrade HF, Teixeira M de M. 2022. Clinical and ECO-Epidemiological aspects of a novel Hyperendemic area of Paracoccidioidomycosis in the Tocantins-Araguaia Basin (northern Brazil), caused by Paracoccidioides SP. J Fungi (Basel) 8:502. https://doi.org/10.3390/jof8050502
57. Heung LJ. 2020. Monocytes and the host response to fungal pathogens. Front Cell Infect Microbiol 10:34. https://doi.org/10.3389/fcimb.2020.00034
58. McEwen JG, Restrepo BI, Salazar ME, Restrepo A. 1987. Nuclear staining of *Paracoccidioides brasiliensis* conidia. J Med Vet Mycol 25:343–345.
59. Seyedmousavi S. 2021. Antifungal drugs. In Abraham DJ (ed), Burger's medicinal chemistry and drug discovery, 8th ed
60. Nguyen TTT, Lee HB. 2022. Discovery of three new *Mucor* species associated with cricket insects in Korea. JoF 8:601. https://doi.org/10.3390/jof8060601
61. Sharifia M, Karimi K, Taherzadeh MJ. 2008. Production of ethanol by filamentous and yeast-like forms of *Mucor indicus* from fructose, glucose, sucrose, and molasses. J Ind Microbiol Biotechnol 35:1253–1259. https://doi.org/10.1007/s10295-008-0422-x
62. Villa F, Cappitelli F, Principi P, Polo A, Sorlini C. 2009. Permeabilization method for in-situ investigation of fungal conidia on surfaces. Lett Appl Microbiol 48:234–240. https://doi.org/10.1111/j.1472-765X.2008.02520.x
63. Zhou X, Ahmed SA, Tang C, Grisolia ME, Warth JFG, Webster K, Peano A, Uhrlass S, Cafarchia C, Hayette MP, Sacheli R, Matos T, Kang Y, de Hoog GS, Feng P. 2023. Human adaptation and diversification in the microsporum canis complex. IMA Fungus 14:14. https://doi.org/10.1186/s43008-023-00120-x
64. Walther G, Pawłowska J, Alastruey-Izquierdo A, Wrzosek M, Rodriguez-Tudela JL, Dolatabadi S, Chakrabarti A, de Hoog GS. 2013. DNA barcoding in *Mucorales*: an inventory of biodiversity. Persoonia 30:11–47. https://doi.org/10.3767/003158513X665070
65. Nguyen TT, Lee HB. 2020. *Mucor cheongyangensis*, a new species isolated from the surface of *lycorma delicatula* in Korea. Phytotaxa 446:33–42. https://doi.org/10.11646/phytotaxa.446.1.4
66. de Souza JI, Pires-Zottarelli CLA, Dos Santos JF, Costa JP, Harakava R. 2012. Isomucor (Mucoromycotina): a new genus from a cerrado reserve in state of Sao Paulo. Mycologia 104:232–241. https://doi.org/10.3852/11-133
67. Hurdeal VG, Gentekaki E, Hyde KD, Nguyen TTT, Lee HB. 2021. Novel *Mucor* species (Mucoromycetes, mucoraceae) from northern Thailand. MycoKeys 84:57–78. https://doi.org/10.3897/mycokeys.84.71530

AUTHOR BIO

Dr. Amir Seyedmousavi is a Senior Staff-Clinical Microbiology Laboratory Director and Faculty member of CPEP Microbiology Fellowship Program at the Department of Laboratory Medicine, Clinical Center, National Institutes of Health, Bethesda, MD, USA. In this role, he works as a Consultant Clinical Microbiologist for Infectious Disease Diagnostic Testing and Hospital Epidemiology Service. He also serves as Director of Mycology and Parasitology sections.He obtained a VMD degree from University of Tehran, Iran, followed by a PhD (cum laude) in Medical Mycology. Then he moved to Netherlands and received a second PhD in Medical Microbiology and Antimicrobial Resistance and completed his Clinical Microbiology Postdoctoral Training and Research at Radboud University Medical Center in Nijmegen. He also conducted postdoctoral research on molecular taxonomy and fungal phylogenetics at Westerdijk Fungal Biodiversity Institute-KNAW in Utrecht, The Netherlands and completed a three-year advanced research fellowship at Molecular Microbiology Section of Laboratory of Clinical Immunology and Microbiology at National Institute of Allergy and Infectious Diseases, Bethesda, MD, USA. He was also previously appointed as an Assistant and Associate Professor of Medical Microbiology/Mycology in Iran.The scientific work in Dr. Seyedmousavi research laboratory focuses on molecular diversity, comparative genomic analysis, epidemiology, infection biology and evolution of antifungal drug resistance of pathogenic opportunistic fungi of human and animal origin. He is also interested in optimization of antifungal therapies through application of pharmacokinetic and pharmacodynamic principles. Another important area is to study new diagnostic technologies such as targeted next-generation sequencing for direct identification of fungi in clinical specimens, and to develop point-of-care testing for detection of fungal infections.He has published over 150 research papers and several book chapters and has delivered over 100 invited lectures. He is co-editor of the textbook Emerging and Epizootic Fungal Infections. He is one of the founding members and coordinator of 'ISHAM Fungal Diagnostics' and 'ISHAM Veterinary Mycology and One Health' working groups.Dr. Seyedmousavi serves as editor for 'Medical Mycology' and 'Medical Mycology Case Reports' the official journals of International Society for Human & Animal Mycology. He is also an associate editor for 'IMA Fungus' and serves on the editorial board of Journal of Clinical Microbiology, and several other peer reviewed journals.He received several prestigious awards including NIH Clinical Center CEO Award in recognition of implementing Candida auris screening for Clinical Center patients. He is also the recipient of the Educational Trust Award from the Journal of Comparative Pathology, due to his significant scientific contributions to the field of Medical Mycology and One Health antimicrobial resistance.